

MULTI ROBOT OPTIMAL TRAJECTORY GENERATION

JOSÉ MAGNO MENDES FILHO^{a,b}, ERIC LUCET^{a,*}^a CEA, LIST, Interactive Robotics Laboratory, Gif-sur-Yvette, F-91191, France^b ENSTA Paristech, Unité d'Informatique et d'Ingénierie des Systèmes, 828 bd des Marechaux, 91762, France* corresponding author: eric.lucet@cea.fr

ABSTRACT.

This paper proposes the real-time implementation of a multi-robot optimal collision-free motion planner algorithm based on a receding horizon approach, for the navigation of a team of mobile robots evolving in an industrial context in presence of different structures of obstacles. The method is validated in simulation environment for a team of three robots. Then, impact of the algorithm parameters setting is studied with regard to critical performance criteria, being mainly real-time implementation, obstacle avoidance and time to complete the task.

KEYWORDS: multi-robot motion planning, nonholonomic mobile robot, decentralized planning, receding horizon.

1. INTRODUCTION

The control of mobile robots is a long-standing subject of research in the iterative robotics domain. As many modern companies started to adopt mobile robot systems such as teams of autonomous forklift trucks [1] to improve their commercial performance, this subject becomes increasingly important and complex. Especially when those robots are executing their tasks in human-occupied environment.

One basic requirement for such robotic systems is the capacity of generating a trajectory that connects two arbitrary configurations. For that, different constraints must be taken into account to ideally find an appropriated trajectory, in particular:

- kinematic and dynamic constraints;
- geometric constraints;
- constraints associated with uncertainties about the current state of world and the outcome of actions.

The first constraints derive directly from the mobile robot architecture implying in nonholonomic constraints for many types of mobile robots. Geometric constraints result from the impossibility of the robots to assume some specific configurations due to the presence of obstacles or environment bounds. In turn, uncertainty constraints come from the impossibility of the robots to have an absolute and complete perception of the world (including their own states) as well as the outcome of non-stochastic events.

We are particularly interest in solving the problem of dynamic planning a trajectory for a team of non-holonomic mobile robots in an partially known environment occupied by static obstacles being near optimal with respect to the execution time (time spent from going from initial to final configurations).

In recent years, a great amount of work towards collision-free trajectory planning has been proposed.

Some work has been done towards analytic methods for solving the problem for certain classes of systems ([]) TODO cite . However [2] shows that analytic methods are inapplicable for nonholonomic systems in presence of obstacles.

Cell decomposition methods as presented in [3] have the downside of requiring a structured configuration space and an *a priori* model of its connectivity. Besides, the cell decomposition reduces the space of admissible solutions. TODO verify/understand.

Initially proposed in [?], the vector field obstacle avoidance method was improve along time for treating problems such as oscillation of the solution for narrow passages. This method does not present a near optimal generated trajectory.

Elastic band approach initially proposed by [?] and extend to mobile manipulators in [? ?] uses approximations of the trajectory shape (combinations of arcs and straight lines) limiting the space of solutions and make this method inappropriate for really constrained environments.

The dynamic window approach [4] can handle trajectory planning for robots at elevated speeds and in presence of obstacles but is not flexible enough to be extended to a multi-robot system.

In this paper, we focus on the development of a motion planning algorithm. This algorithm finds collision-free trajectories for a multi-robot system in presence of static obstacles which are perceived by the robots as they evolve in the environment. The dynamic trajectories found are near optimal with respect to the total time spend going from the initial configuration to the final one. Besides, this algorithm uses a decentralized approach making the system more robust to communication outages and individual robot failure than compared to a centralized approach. Identified drawbacks are the dependence on several parameters for achieving real-time perfor-

mance and good solution optimality, and not being able to handle dynamic obstacles as it is.

This algorithm is based mainly on the work done in [5] but we made changes in particular to respect a precise final configuration for the multi-robot system and about how to set parameters for solving the nonlinear programming problem (NLP).

This paper is structured as follows: The second section presents a trajectory planning algorithm that solves the problem of one robot going from an initial configuration to a final one in the presence of static obstacles. The third section extends the method presented in the second section so a collision-free trajectory that maintains the communication link between the robots in the team can be computed. The fourth section is dedicated to the results found by this method and the analysis of the computation time and solution quality and how they are impacted by the algorithm parameters. The fifth section presents the comparison of this approach to another one presented in [1]. Finally, in section six we present our conclusions and perspectives.

2. PROBLEM STATEMENT

2.1. ASSUMPTIONS

In the development of this approach the following assumptions are made:

- (1.) The motion of the multi-robot system begins at the instant t_{init} and goes until the instant t_{final} .
- (2.) The team of robots consists of a set \mathcal{R} of B non-holonomic mobile robots.
- (3.) A robot (denoted R_b , $R_b \in \mathcal{R}$, $b \in \{0, \dots, B-1\}$) is geometrically represented by a circle of radius ρ_b centered at (x_b, y_b) .
- (4.) All obstacles in the environment are considered static. They can be represented by a set \mathcal{O} of M static obstacles.
- (5.) An obstacle (denoted O_m , $O_m \in \mathcal{O}$, $m \in \{0, \dots, M-1\}$) is geometrically represented either as a circle or as a convex polygon. In the case of a circle its radius is denoted r_{O_m} centered at (x_{O_m}, y_{O_m}) .
- (6.) For a given instant $t_k \in [t_{init}, t_{final}]$, any obstacle O_m having its geometric center apart from the geometric center of the robot R_b of a distance inferior than the detection radius $d_{b, sen}$ of the robot R_b is considered detected by this robot. Thus, this obstacle is part of the set \mathcal{O}_b ($\mathcal{O}_b \subset \mathcal{O}$) of detected obstacles.
- (7.) A robot has precise knowledge of the position and geometric representation of a detected obstacle.
- (8.) A robot can access information about any robot in the team using a wireless communication link.

- (9.) Latency, communication outages and other problems associated to the communication between robots in the team are neglected.

- (10.) Dynamics was neglected.

- (11.) The input of a mobile robot R_b is limited.

2.2. CONSTRAINTS AND COST FUNCTIONS

After loosely defining what is the motion planning problem in Section 1 and presenting the assumptions in the previous Subsection we can identify and define what are the constraints and the cost function for the multi-robot navigation.

- (1.) The solution of the motion planning problem for the robot R_b represented by the pair $(q_b^*(t), u_b^*(t)) - q_b^*(t) \in \mathbb{R}^n$ being the solution trajectory for the robot's configuration and $u_b^*(t) \in \mathbb{R}^p$ the solution trajectory for the robot's input - must satisfy the robots kinematic model equation:

$$\dot{q}_b^*(t) = f(q_b^*(t), u_b^*(t)), \quad \forall t \in [t_{init}, t_{final}]. \quad (1)$$

- (2.) The planned initial configuration and initial input for the robot R_b must be equal to the initial configuration and initial input of R_b :

$$q_b^*(t_{init}) = q_{b,init}, \quad (2)$$

$$u_b^*(t_{init}) = u_{b,init}. \quad (3)$$

- (3.) The planned final configuration and final input for the robot R_b must be equal to the goal configuration and goal input for R_b :

$$q_b^*(t_{final}) = q_{b,goal}, \quad (4)$$

$$u_b^*(t_{final}) = u_{b,goal}. \quad (5)$$

- (4.) The practical limitations of the input impose the following constraint: $\forall t \in [t_{init}, t_{final}], \forall i \in [1, 2, \dots, p]$,

$$|u_{b,i}^*(t)| \leq u_{b,i,max}. \quad (6)$$

- (5.) The cost for the multi-robot system navigation is defined as:

$$L(q(t), u(t)) = \sum_{b=0}^{B-1} L_b(q_b(t), u_b(t), q_{b,goal}, u_{b,goal}) \quad (7)$$

where $L_b(q_b(t), u_b(t), q_{b,goal}, u_{b,goal})$ is the integrated cost for one robot motion planning (see [6]).

- (6.) To ensure collision avoidance with obstacles the euclidean distance between a robot and an obstacle (denoted $d(R_b, O_m) \mid O_m \in \mathcal{O}_b, R_b \in \mathcal{B}$) has to satisfy:

$$d(R_b, O_m) \geq 0. \quad (8)$$

For the circle representation of an obstacle the distance $d(R_b, O_m)$ is defined as:

$$\sqrt{(x_b - x_{O_m})^2 + (y_b - y_{O_m})^2} - \rho_b - r_{O_m}.$$

For the polygon representation, the distance was calculated using three different definitions according to the Voronoi region [7] R_b is located. Figure 1 shows an example of the three kinds of regions for a quadrilateral $ABCD$ representation. The Voronoi regions are defined by the lines containing the sides (s lines) and by the lines passing through the vertices that are orthogonal to the sides (r lines).

In this example, the region in which the robot R_b is located at an instant t_k can be computed by evaluating the line equations $s_{AB}, s_{BC}, s_{CD}, s_{DA}, r_{AB}, r_{AD}, r_{BA}, r_{BC}, r_{CB}, r_{CD}, r_{DC}$ and r_{DA} for the position associated with the configuration $q_b^*(t_k)$.

TODO: for the quadrilateral we have 9 regions, the 3 that shown...

In addition, the distance robot-to-quadrilateral could be found as follows:

(a) If robot in region 1:

$$\sqrt{(x_b - x_A)^2 + (y_b - y_A)^2} - \rho_b$$

which is simply the distance of the robot to the vertex A .

(b) If robot in region 2:

$$d(s_{DA}, (x_b, y_b)) - \rho_b$$

where

$$d(s_{DA}, (x_b, y_b)) = \frac{|a_{s_{DA}}x_b + b_{s_{DA}}y_b + c_{s_{DA}}|}{\sqrt{a_{s_{DA}}^2 + b_{s_{DA}}^2}}.$$

The distance $d(s_{DA}, (x_b, y_b))$ represents the distance from the robot to the side DA .

(c) If robot in region 3:

$$-\min(d(s_{AB}, (x_b, y_b)), \dots, d(s_{DA}, (x_b, y_b))) - \rho_b$$

which represents the amount of penetration of the robot in the obstacle.

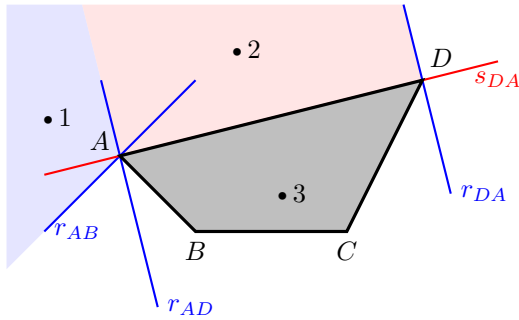


FIGURE 1. Voronoi regions used for case differentiation.

(7.) In order to prevent inter-robot collisions the following constraint must be respected: $\forall (R_b, R_c) \in \mathcal{R} \times \mathcal{R}, b \neq c, c \in \mathcal{C}_b$,

$$d(R_b, R_c) - \rho_b - \rho_c \geq 0 \quad (9)$$

where $d(R_b, R_c) = \sqrt{(x_b - x_c)^2 + (y_b - y_c)^2}$ and \mathcal{C}_b is the set of robots that present a collision risk with R_b .

(8.) Finally, the need of a communication link between two robots (R_b, R_c) yields to the following constraint:

$$d(R_b, R_c) - \min(d_{b,com}, d_{c,com}) \leq 0 \quad (10)$$

with $d_{b,com}, d_{c,com}$ the communication link reach of each robot and \mathcal{D}_b is the set of robots that present a communication lost risk with R_b .

3. DISTRIBUTED MOTION PLANNING

3.1. RECEDING HORIZON APPROACH

As said before trying to find the solution from the initial configuration until the goal is not feasible. Thus, the planning has to be computed on-line as the multi-robot system evolves in the environment. One way to do so is to use a receding horizon control approach [8].

All robots in the team use the same constant planning horizon T_p and update horizon T_c . T_p is the time horizon for which a solution will be computed, T_c is the time horizon during which a plan is executed while the next plan, for the next timespan T_p , is being computed.

For each receding horizon planning problem the following is done:

Step 1. Compute an intended solution trajectory (denoted $(\hat{q}_b(t), \hat{u}_b(t))$) by ignoring coupling constraints, i. e., constraints 9 and 10 that involve other robots in the team.

Step 2. Robots involved in a conflict (collision or lost of communication) update their trajectories by solving another constrained optimization problem that take into account coupling constraints (9 and 10). This is done by using the other robots' intended trajectories computed in the previous step as an estimative of the robots final trajectories. If a robot is not involved in any conflict its final solution trajectory is identical to the one estimated in the Step 1.

This scheme is explained in details in [5] where the receding horizon optimization problems are formulated based on the constraints and cost function defined in Section 2.

However, constraints related to the goal configuration and input of the motion planning problem are neglected in the receding horizon scheme presented in [5]. The constraints 4 and 5 are not considered in the receding horizon optimization problems. For that, a termination procedure is proposed in the following that enables the robots to reach their goal state.

3.2. MOTION PLANNING TERMINATION

As the robots evolve their states approximate to the goal states. But simply stopping the motion planner as the robots are in the neighbourhood of their final

3.3. STRATEGIES FOR SOLVING THE CONSTRAINED OPTIMIZATION PROBLEMS

3.3.1. FLATNESS PROPERTY

As explained in [5] all mobile robots consisting of a solid block in motion can be modelled as a flat system. This means that a change of variables is possible in a way that states and inputs of the kinematic model of the mobile robot can be written in terms of the new variable, called flat output (z), and its l th first derivatives. Thus, the behaviour of the system can be completely determined by the flat output.

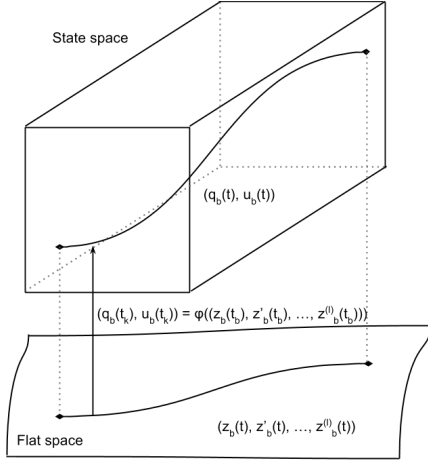


FIGURE 3. Flatness

Searching for a solution to our problem in the flat space rather than in the actual configuration space of the system present advantages. It prevents the need for integrating the differential equations of system and reduces the dimension of the problem of finding an optimal admissible trajectory. After finding (optimal) trajectories in the flat space it is possible to retrieve back the original configuration and input trajectories as shown in Figure 3.

3.3.2. PARAMETRIZATION OF THE FLAT OUTPUT BY B-SPLINES

Another important aspect of this approach is the parametrization of the flat output trajectory. As done in [?] the use of B-spline functions present interesting properties:

- It is possible to specify a level of continuity C^k when using B-splines without additional constraints.
- B-spline presents a local support, i.e., changes in parameters values have a local impact on the resulting curve.

The first property is very well suited for parametrizing the flat output since its l th first derivatives will be needed when computing the system actual state and input trajectories. The second property is important when searching for an admissible solution in the flat space; such parametrization is more efficient

and well-conditioned than, for instance, a polynomial parametrization.

3.3.3. OPTIMIZATION SOLVER

There is a variety of numerical optimization packages implemented in many different programming languages available for solving optimization problems [9].

Obviously not all of those implementations are suited for solving the particular kind of optimization problems presented before.

As explained in ?? a Feasible Sequential Quadratic Programming is best suited for solving the motion planning problem as stated in this paper. This class of solvers compute at every iteration solution that respects the problem constraints.

TODO keep explaining, present SLSQP and ALGENCAN, present reasons why we used SLSQP (i.e. availability in python, free license, and faster than ALGENCAN)

SLSQP numerical stability

4. SIMULATION RESULTS

Here we show the results and analyses founded for the motion planner presented in the previous sections.

The trajectory and velocities shown in the Figures 4 and 5 illustrate a motion planning solution found for a team of three robots. The robots move in an environment where three static obstacles are present. Each point along the trajectory line of a robot represents the beginning of a T_c computation horizon.

In Figure 4 we show the resulting plan when coupling constraints are ignored (Step 2 is not performed). In Figure 5 we have a collision-free solution. Notice the changes in the trajectories and velocities resulting from the solution update.

The performance and solution quality of the motion planning algorithm previously presented depends on several parameters. These parameters can be split into two groups. The **algorithm related** parameters and the **optimization solver related** ones. Among the former group, the most important ones are:

- The number of sample for time discretization (N_s);
- The number of internal knots for the B-splines curves (n_{knots});
- The planning horizon for the sliding window (T_p);
- The computation horizon (T_c).

The latter kind depends on the optimization solver adopted. However, since most of them are iterative methods, it is common to have at least the two following parameters:

- Maximum number of iterations;
- Stop condition.

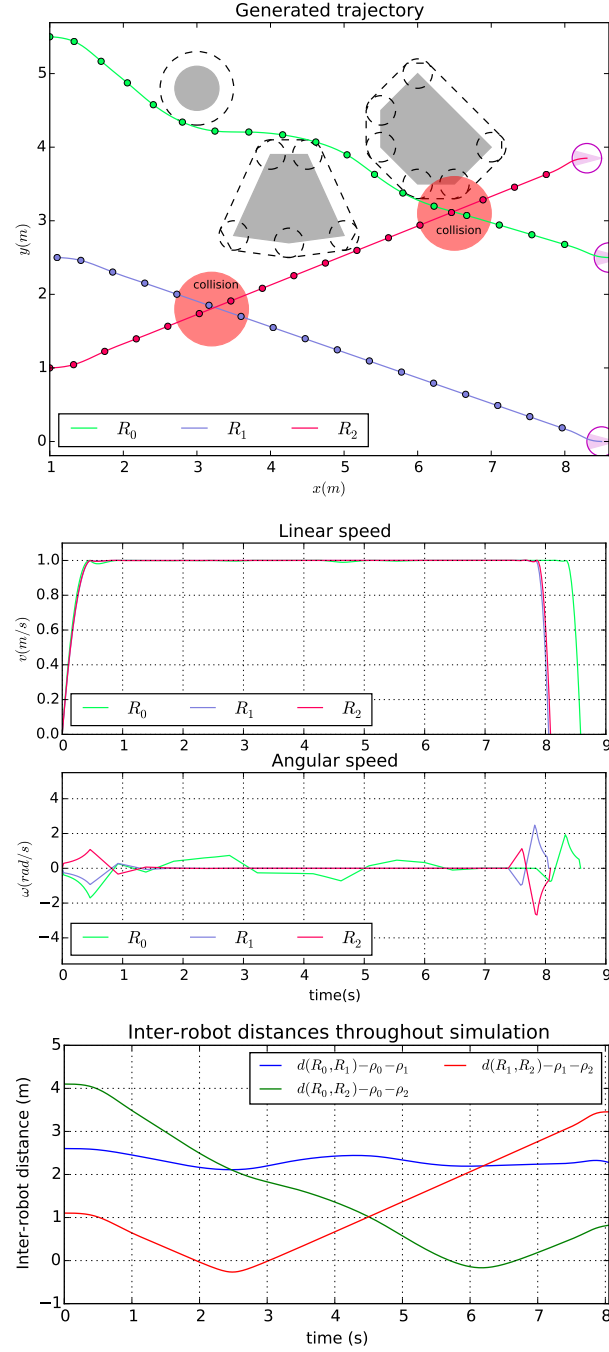


FIGURE 4. Motion planning without collision handling

This high number of parameters having influence on the solution and/or on the time for finding a solution makes the search for a satisfactory set of parameters' values a laborious task.

Thus, it is important to have a better understanding of how some performance criteria are impacted by the changes in algorithm parameters.

4.1. PARAMETERS' IMPACT ANALYSES

Three criteria considered important for the validation of this method were studied. We tested different parameters configuration and scenario in order to un-

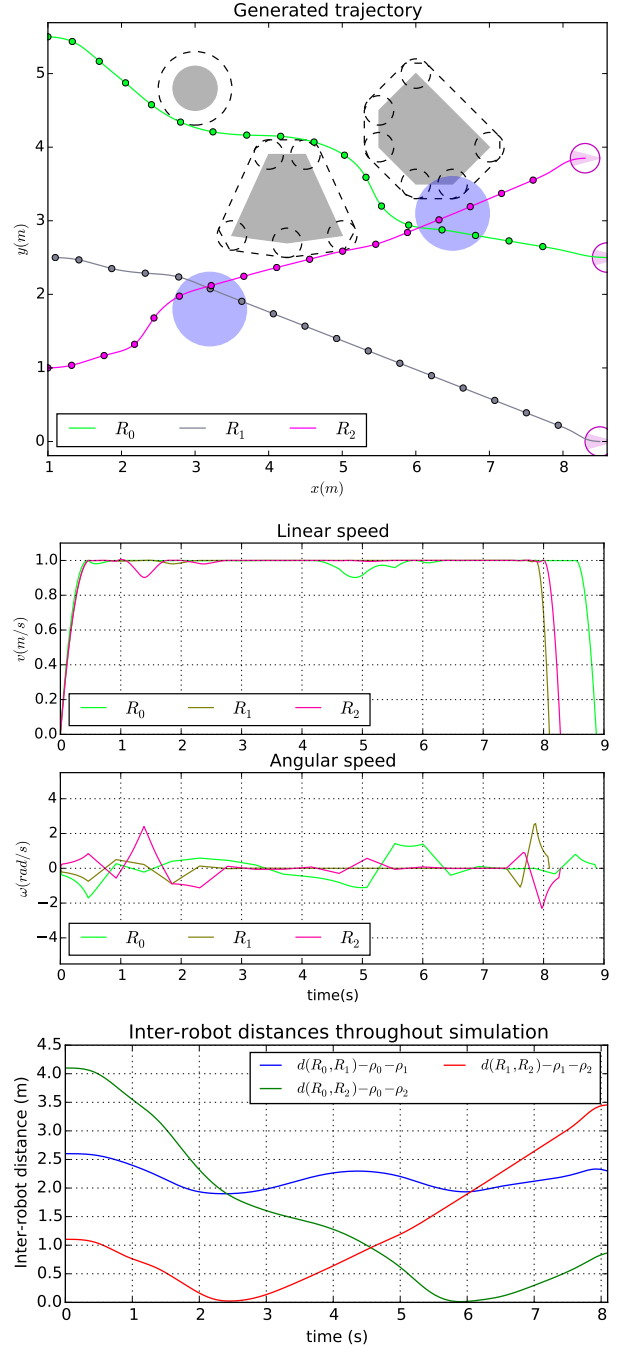


FIGURE 5. Motion planning solution with collision handling

derstand how they influence those criteria. The three criteria defined for a given robot R_b are:

- *Maximum computation time* over the computation horizon (MCT/T_c ratio).
- *Obstacle penetration area* (P).
- *Total execution time* (T_{tot}).

4.1.1. DETECTION RADIUS IMPACT

As the detection radius of the robot increases more obstacles are seen at once which, in turn, increases the number of constraints in the optimization problems.

The impact of increasing the detection radius $d_{b, \text{sen}}$ in the computation performance (*Maximum computation time* over computation horizon MCT/T_c) can be seen in the Figure 6 for a scenario where seven obstacles were present. Naturally, the computation time stops increasing as the robot sees all obstacles present in the environment.

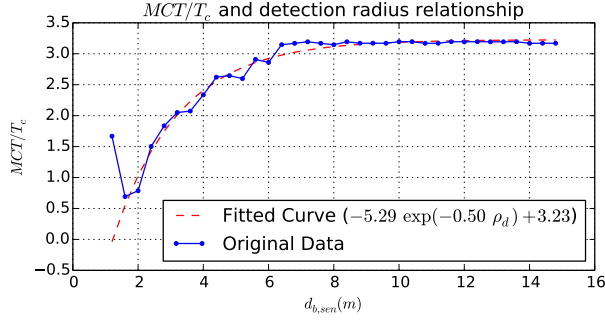


FIGURE 6. Increasing of detection radius and impact on a MCT/T_c ratio

Furthermore, the Figure 7 shows how the time total execution time decreases as the radius increases pointing out how a better knowledge of the environment produces a better solution in terms of T_{tot} time.

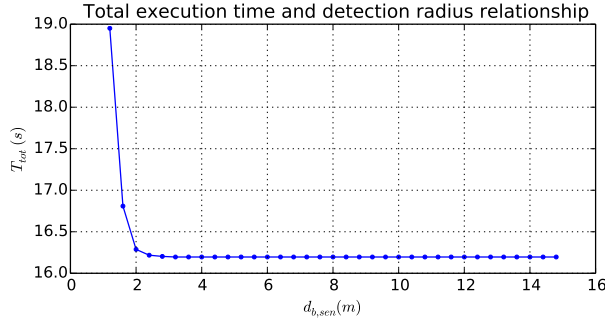


FIGURE 7. Increasing of detection radius and impact on a T_{tot} ratio

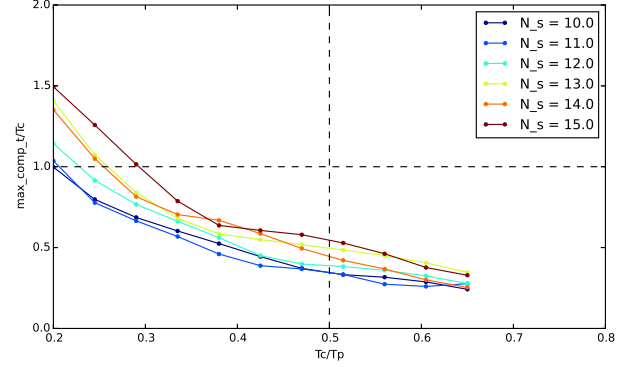
These two behaviours point how a compromise between computation time and optimality must be found.

4.2. MAXIMUM COMPUTATION TIME OVER COMPUTATION HORIZON MCT/T_c

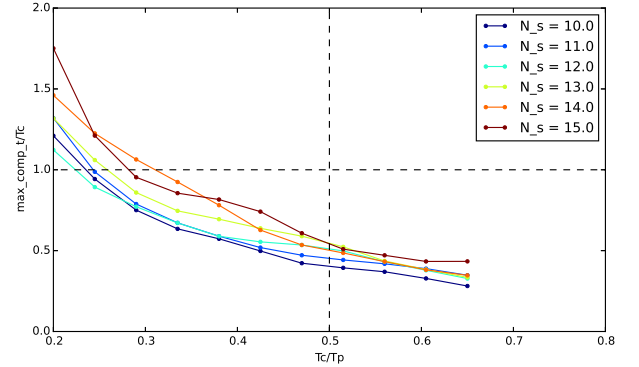
The significance of this criterion lays in the need of quarantining the real-time property of this algorithm. In a real implementation of this approach the computation horizon would have always to be superior than the maximum time took for computing a planning section (coupling constraints taken into account).

Based on several simulations with different scenarios we were able to produce the charts shown in the Figure 8

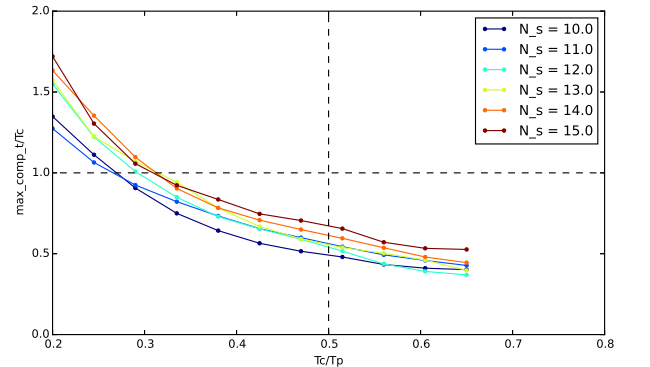
- SLSPQ method request $O(n^3)$ time, n being the number of knots;



(A) . Four internal knots. Average variance between lines is 1.047×10^{-2}



(B) . Five internal knots. Average variance between lines is 0.972×10^{-2}



(C) . Six internal knots. Average variance between lines is 0.587×10^{-2}

FIGURE 8. Three obstacles scenario

4.3. OBSTACLE PENETRATION P

?? TODO rescale images

4.4. TOTAL EXECUTION TIME T_{tot}

TODO Comparison with the other method;

TODO Before concluding do comparison with other approach and make sure to have multi-robot stuff

5. CONCLUSIONS

TODO perspectives

Analise influence of dynamics of system, sensors, communication latency;

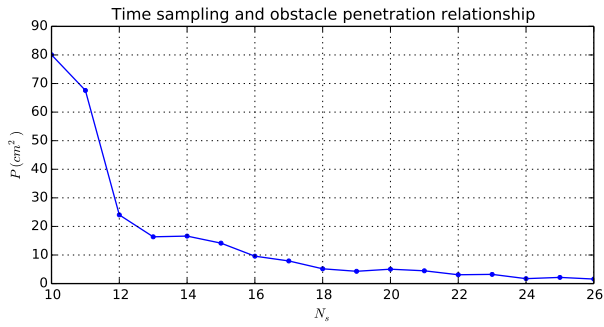


FIGURE 9. Obstacle penetration decreasing as sampling increases

REFERENCES

- [1] Autonomous robots are helping to pack your amazon orders. <http://www.gizmag.com/amazon-kiva-fulfillment-system/34999/>. Accessed: 2015-07-07.
- [2] J. T. Schwartz, M. Sharir. A survey of motion planning and related geometric algorithms. *Artificial Intelligence* **37**(1):157–169, 1988.
- [3] J.-C. Latombe. *Robot motion planning*, vol. 124. Springer Science & Business Media, 2012.
- [4] D. Fox, W. Burgard, S. Thrun, et al. The dynamic window approach to collision avoidance. *IEEE Robotics & Automation Magazine* **4**(1):23–33, 1997.
- [5] M. Defoort. Contributions à la planification et à la commande pour les robots mobiles coopératifs. *Ecole Centrale de Lille* 2007.
- [6] M. Defoort, A. Kokosy, T. Floquet, et al. Motion planning for cooperative unicycle-type mobile robots with limited sensing ranges: A distributed receding horizon approach. *Robotics and Autonomous Systems* **57**(11):1094–1106, 2009. doi:10.1016/j.robot.2009.07.004.
- [7] C. Ericson. *Real-Time Collision Detection*. M038/the Morgan Kaufmann Ser. in Interactive 3D Technology Series. Taylor & Francis, 2004.
- [8] T. Keviczky, F. Borrelli, G. J. Balas. Decentralized receding horizon control for large scale dynamically decoupled systems. *Automatica* **42**(12):2105–2115, 2006. doi:10.1016/j.automatica.2006.07.008.
- [9] R. E. Perez, P. W. Jansen, J. R. R. A. Martins. pyOpt: A Python-based object-oriented framework for nonlinear constrained optimization. *Structures and Multidisciplinary Optimization* **45**(1):101–118, 2012. doi:10.1007/s00158-011-0666-3.